


Crystal structure of minocycline hydrochloride dihydrate form A, C₂₃H₂₈N₃O₇Cl (H₂O)₂

Austin M. Wheatley,¹ James A. Kaduk ^{1,2,a)} Amy M. Gindhart,³ and Thomas N. Blanton³

¹North Central College, 131 S. Loomis St., Naperville, Illinois 60540

²Illinois Institute of Technology, 3101 S. Dearborn St., Chicago, Illinois 60616

³ICDD, 12 Campus Blvd., Newtown Square, Pennsylvania 19073-3273

(Received 13 May 2018; accepted 17 September 2018)

The crystal structure of minocycline hydrochloride dihydrate has been solved and refined using synchrotron X-ray powder diffraction data, and optimized using density functional techniques. Minocycline hydrochloride dihydrate crystallizes in space group $P2_12_12_1$ (#19) with $a = 7.40772(1)$, $b = 14.44924(3)$, $c = 22.33329(4)$ Å, $V = 2390.465(12)$ Å³, and $Z = 4$. The minocycline cation is a zwitterion: both dimethylamino groups are protonated and one hydroxyl group is ionized. A potential ambiguity in the orientation of the amide group was resolved by considering Rietveld refinement residuals and displacement coefficients, as well as DFT energies. The crystal structure is dominated by hydrogen bonds. Both water molecules and a hydroxyl group act as donors to the chloride anion. Both protonated dimethyl amine groups act as donors to the ionized hydroxyl group. Several intramolecular O–H···O hydrogen groups help determine the conformation of the cation. The powder pattern is included in the Powder Diffraction File™ as entry 00-066-1606. © 2018 International Centre for Diffraction Data. [doi:10.1017/S0885715618000787]

Key words: minocycline hydrochloride dihydrate, Minocin[®], powder diffraction, Rietveld refinement, density functional theory

I. INTRODUCTION

Minocycline hydrochloride dihydrate (brand names Minocin[®] oral suspension and Dynacin[®] anhydrous tablets) is a semisynthetic tetracycline that functions primarily as a bacteriostatic antibiotic (Bstatic), which is a biochemical agent that exerts its antimicrobial effects through the inhibition of protein synthesis, DNA replication, and/or other phases of bacterial cellular metabolism; thus, inhibiting the bacterial growth and reproductive cycle, without killing the bacteria. Minocin is commonly used in the treatment of bacterial infections (Gram-positive, Gram-negative, and other bacterial microorganisms), rheumatoid arthritis, skin or soft tissue infection, trachoma (eye infection), and several other bacterial-causing diseases. Minocin often is considered when penicillin is contraindicated and is utilized as an alternative option only to treat or prevent infections caused by susceptible strains of microorganisms. The IUPAC name (CAS Registry number 128420-71-3) is (4*S*,4*aS*,5*aR*,12*aS*)-4,7-*bis* (dimethylamino)-3,10,12,12*a*-tetrahydroxy-1,11-dioxo-1,4,4-*a*,5,5*a*,6,11,12*a*-octahydro-tetracene-2-carboxamide hydrochloride dihydrate. A two-dimensional molecular diagram is shown in Figure 1.

Three crystalline polymorphs of minocycline base, as well as a process for producing amorphous minocycline, are claimed in US patent application 2010/0286417 (Mendes *et al.*, 2010). Chinese patent CN101693669B (Xiurong *et al.*, 2012) claims Form A of minocycline hydrochloride

hydrate, and discloses Form B. Form A crystallizes in $P2_12_12_1$, with $a = 7.405(3)$, $b = 14.452(5)$, $c = 22.315(8)$ Å, $V = 2388.28$ Å³, and $Z = 4$. Form B crystallizes in $P3_121$ with $a = 13.143$, $c = 27.417(7)$ Å, $V = 4101.85$ Å³, and $Z = 6$. A powder pattern for “ α -minocycline hydrochloride” (which corresponds to Form A of the Chinese patent) is reported in Rodrigues *et al.* (2014), as well as a new β polymorph.

This work was carried out as part of a project (Kaduk *et al.*, 2014) to determine the crystal structures of large-volume commercial pharmaceuticals, and include high-quality powder diffraction data for these pharmaceuticals in the Powder Diffraction File (Fawcett *et al.*, 2017).

II. EXPERIMENTAL

Minocycline hydrochloride dihydrate was a commercial reagent, purchased from USP (Lot #R01680), and was used as-received. The yellow powder was packed into a 1.5 mm diameter Kapton capillary, and rotated during the measurement at ~50 Hz. The powder pattern was measured at 295 K at beam line 11-BM (Lee *et al.*, 2008; Wang *et al.*, 2008) of the Advanced Photon Source at Argonne National Laboratory using a wavelength of 0.414163 Å from 0.5 to 50° 2θ with a step size of 0.001° and a counting time of 0.1 s step⁻¹.

The pattern was indexed on a primitive orthorhombic unit cell with $a = 7.405$, $b = 14.456$, $c = 22.340$, $V = 2391.4$ Å³, and $Z = 4$ using DICVOL as incorporated into FOX (Favre-Nicolin and Černý, 2002). A reduced cell search in the Cambridge Structural Database (Groom *et al.*, 2016) combined with the chemistry C, H, N, O, and Cl only yielded one

^{a)} Author to whom correspondence should be addressed. Electronic mail: kaduk@polycrystallography.com

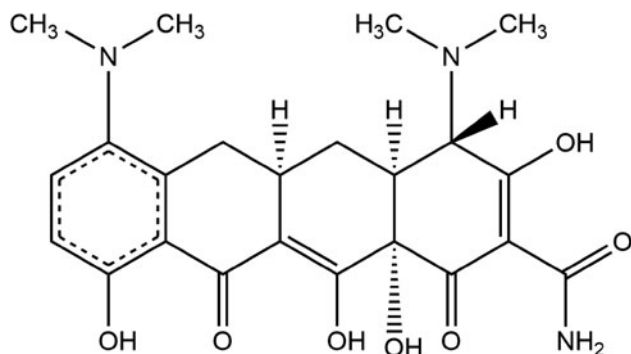


Figure 1. The molecular structure of minocycline (PDB ligand MIY).

hit, but no crystal structure for a minocycline derivative. Analysis of the systematic absences suggested the space group $P2_12_12_1$ (#19), which was confirmed by successful solution and refinement of the structure. The structure was solved by direct methods using EXPO2014 (Altomare *et al.*, 2013). Some atom types were reassigned manually based on the known connectivity of the molecule. The structure solution yielded the opposite stereoisomer to the known structure. The molecule was inverted using EXPGUI (Toby, 2001).

Rietveld refinement was carried out using GSAS (Toby, 2001; Larson and Von Dreele, 2004). Only the $1.8\text{--}25.0^\circ$ portion of the pattern was included in the refinement ($d_{\text{min}} = 0.957 \text{ \AA}$). All non-H bond distances and angles were subjected to restraints, based on a Mercury/Mogul Geometry Check (Bruno *et al.*, 2004; Sykes *et al.*, 2011) of the molecule. The Mogul average and standard deviation for each quantity were used as the restraint parameters. The restraints

contributed 0.75% to the final χ^2 . The hydrogen atoms were included in calculated positions, which were recalculated during the refinement using Materials Studio (Dassault, 2016). Positions of the active hydrogens were derived by analysis of potential hydrogen bonding patterns. A common U_{iso} was refined for the non-H atoms of the fused-ring system, another U_{iso} for the ring-substituent oxygen atoms, another for the nitrogen and carbons for the other substituents, and a common U_{iso} for the water molecules. The U_{iso} for O7 and N12 of the amide group were refined independently. The U_{iso} for each hydrogen atom was constrained to be $1.3\times$ that of the heavy atom to which it is attached. The peak profiles were described using profile function #4 (Thompson *et al.*, 1987; Finger *et al.*, 1994), which includes the Stephens (1999) anisotropic strain broadening model. The background was modeled using a two-term shifted Chebyshev polynomial, with a seven-term diffuse scattering function to model the Kapton capillary and any amorphous component.

The structure was also solved with FOX, using the MIY ligand from the Protein Data Bank (Berman *et al.*, 2000) and a Cl atom as fragments. This structure (experimental from complexes with proteins) was used because of the variability in the minocycline structures among the various online sources. The oxygen atoms of the two water molecules were located in a difference Fourier map. The conformation of the amide group was opposite to that from the direct methods solution. Refinements were carried out on both models. The simulated annealing model yielded poorer residuals (reduced $\chi^2 = 4.943$ vs. 3.820 for the direct methods model) and an energy $16.0 \text{ kcal mol}^{-1}$ higher, so this model was discarded.

The final refinement of 141 variables using 23293 observations (23200 data points and 93 restraints) yielded the

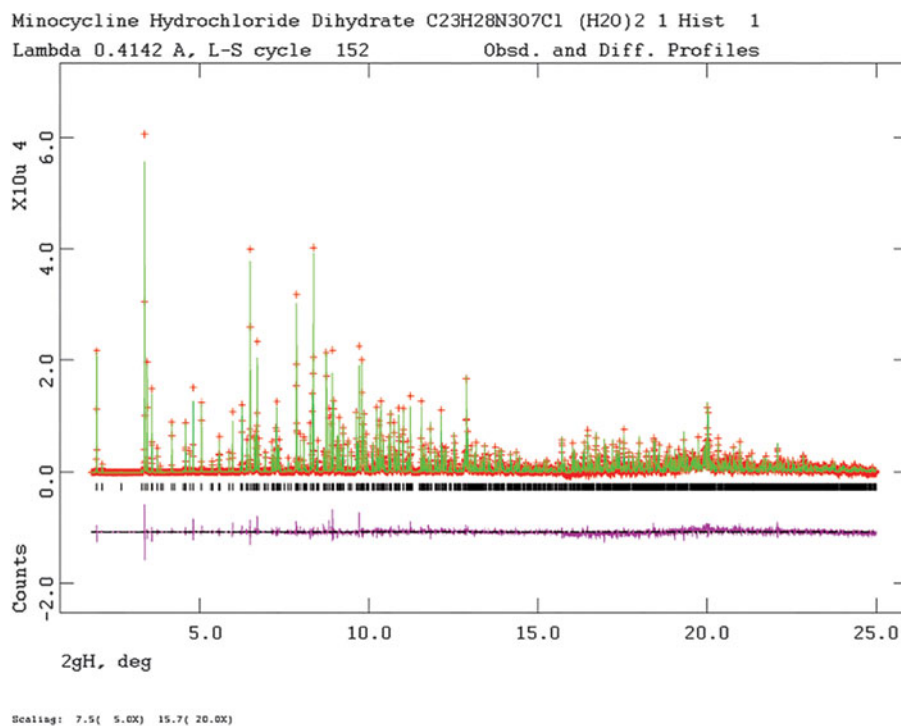


Figure 2. (Color online) The Rietveld plot for the refinement of minocycline hydrochloride dihydrate. The red crosses represent the observed data points, and the green line is the calculated pattern. The blue curve is the difference pattern, plotted at the same vertical scale as the other patterns. The vertical scale has been multiplied by a factor of 5 for $2\theta > 7.5^\circ$, and by a factor of 20 for $2\theta > 15.7^\circ$.

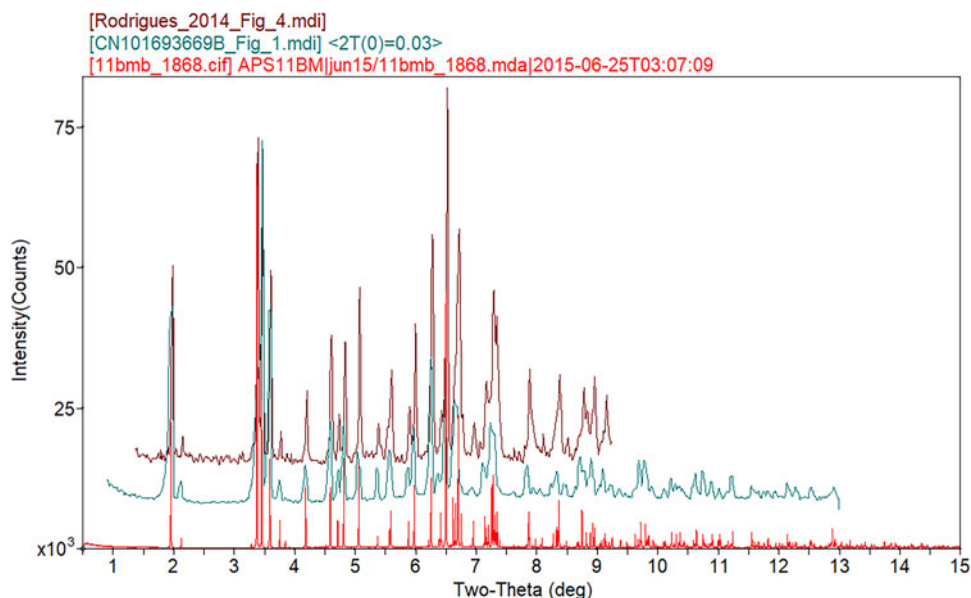


Figure 3. (Color online) Comparison of the synchrotron pattern to that of minocycline hydrochloride dihydrate from Figure 1 of Chinese Patent Application 101693669B (reported as hydrate) and Figure 4 from Rodrigues *et al.* (2014). The Literature patterns (measured using CuK α radiation) were digitized using UN-SCAN-IT, and re-scaled to the synchrotron wavelength of 0.414163 Å using Jade 9.8.

residuals $R_{wp} = 0.0869$, $R_p = 0.0708$, and $\chi^2 = 3.820$. The largest peak (1.55 Å from H46) and hole (1.63 Å from C23) in the difference Fourier map were 0.58 and -0.58 eÅ^{-3} , respectively. The Rietveld plot is included as Figure 2. The largest errors in the fit are in the shapes of some of the strong, low angle peaks.

A density functional geometry optimization (fixed experimental unit cell) was carried out using VASP (Kresse and Furthmüller, 1996). The calculation used the GGA-PBE functional, a plane wave cut-off energy of 400.0 eV, and a k -point spacing of 0.5 Å^{-1} leading to a $2 \times 1 \times 1$ mesh. A density functional geometry optimization was also carried out using CRYSTAL14 (Dovesi *et al.*, 2014). The basis sets for the H, C, N, and O atoms were those of Gatti *et al.* (1994), and the basis set for chlorine was that of Peintinger *et al.* (2013). The calculation was run on eight 2.1 Ghz Xeon cores (each with 6 GB RAM) of a 304-core Dell Linux cluster at Illinois Institute of Technology, using 8 k -points and the B3LYP functional, and took ~ 82 h.

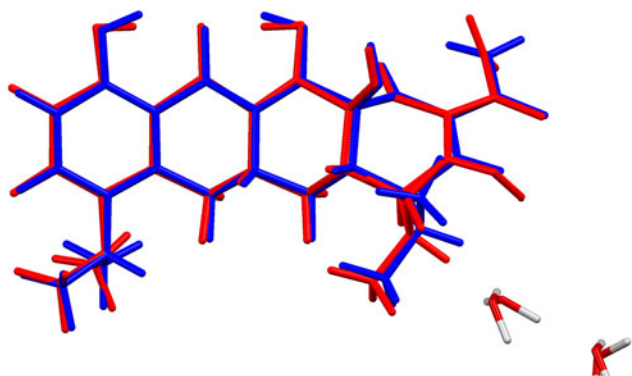


Figure 4. (Color online) Comparison of the refined and optimized (CRYSTAL14) structures of the cation in minocycline hydrochloride dihydrate. The Rietveld refined structure is in red, and the DFT-optimized structure is in blue.

III. RESULTS AND DISCUSSION

The experimental powder pattern of minocycline hydrochloride dihydrate matches those of Form A from Xiurong *et al.* (2012) and that of “ α -minocycline hydrochloride” from Rodrigues *et al.* (2014) well enough to conclude that the materials are the same (Figure 3). The material studied by Rodrigues *et al.* (2014) was also a commercial sample, so we can conclude that the material studied here is representative of that actually used in the market.

The refined atom coordinates of minocycline hydrochloride dihydrate and the coordinates from the DFT optimizations are reported in the CIFs attached as Supplementary Material. The root-mean-square Cartesian displacement of the non-hydrogen atoms in the minocycline cations is 0.094 Å (Figure 4). The largest deviation is 0.210 Å at C30. The excellent agreement between the refined and optimized structures is evidence that the experimental structure is correct (van de Streek and Neumann, 2014). The optimized structures from VASP and CRYSTAL14 are compared in Figure 5. The structures are almost identical. The RMSD is only 0.0456 Å and the maximum displacement is 0.1339 Å . The major difference was in the orientation of the methyl group C34. This discussion concentrates on the CRYSTAL14-optimized structure. The asymmetric unit (with atom numbering) is illustrated in Figure 6, and the crystal structure is presented in Figure 7.

In MIY, O6 is identified as a hydroxyl group, and it was included in the initial Rietveld refinement as O6–H67. The O6 \cdots N9 intermolecular distance was 2.608 Å , ideally oriented to form a hydrogen bond. In both DFT calculations, H67 moved to protonate N9. Rodrigues *et al.* (2014) indicate that both dimethylamine groups are protonated in α -minocycline hydrochloride dihydrate, consistent with this observation. In the solid state, the minocycline cation occurs in a different configuration than is usually pictured: the cation is a zwitterion. The C33–O6 distance (1.254 Å from VASP and 1.247 Å from CRYSTAL14) is smaller than the average phenyl–O $^-$ distance of $1.304(44) \text{ Å}$ from 4519 hits in the CSD

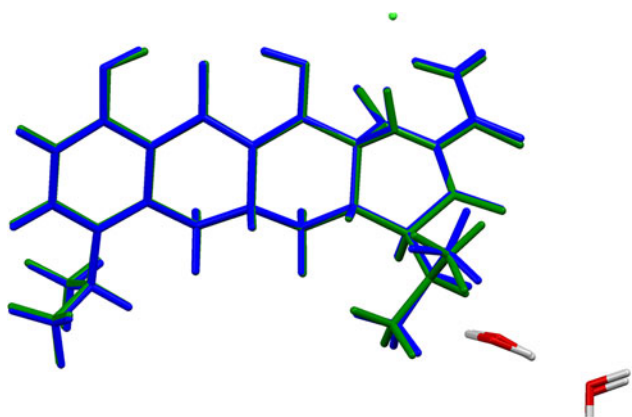


Figure 5. (Color online) Comparison of the VASP (green) and CRYSTAL14 (blue) optimized structures of the minocycline cation.

(Groom *et al.*, 2016) (Figure 8). The difference is only -1.2 esd, so the distance is reasonable.

There is a potential ambiguity in the orientation of the amide group O7/N12. Direct methods suggested the orientation presented here, while simulated annealing yielded the opposite orientation. The current orientation yielded lower refinement residuals and a lower DFT energy. The displacement coefficients of O7 and N12 were refined independently to values of 0.0708(12) and 0.0662(27), respectively. The difference is only 1.6 esd helping to confirm the atom identifications.

Almost all of the bond distances, bond angles, and torsion angles fall within the normal ranges indicated by a Mercury Mogul Geometry Check (Macrae *et al.*, 2008). The O3–C17 distance of 1.296 Å [average = 1.228(21), Z -score = 3.2] is flagged as unusual. This carbonyl group acts as an acceptor in two intramolecular O–H \cdots O hydrogen bonds, and is longer than normal, but is not an unreasonable distance. The O5–C27–C22 angle of 106.3° [average = 110.1(12), Z -score = 3.1]

is flagged as unusual. The Z -score is the result of the small ESD on the average.

Quantum chemical geometry optimizations (DFT/6-31G*/water) using Spartan '16 (Wavefunction, 2017) indicated that the observed conformation of minocycline in minocycline hydrochloride dihydrate is 8.1 kcal mole $^{-1}$ higher in energy than the local minimum energy conformation. The differences are in the orientations of the protonated dimethylamine groups and the amide suggesting that intermolecular interactions contribute to the observed conformation of the molecule. Attempts to perform molecular mechanics conformational analysis yielded “folded” conformations with the tetracycline bent around the C19–C21 axis.

Analysis of the contributions to the total crystal energy using the Forcite module of Materials Studio (Dassault, 2016) suggests that angle, bond, and torsion distortion terms are significant in the intramolecular deformation energy, as might be expected from a fused ring system. The intermolecular energy contains significant contributions from van der Waals repulsions and electrostatic attractions, which in this force-field-based analysis include hydrogen bonds. The hydrogen bonds are better analyzed using the results of the DFT calculation.

Both water molecules act as donors in O–H \cdots Cl hydrogen bonds to the chloride anion (Table I). The energies of these hydrogen bonds were calculated using the correlation from Kaduk (2002). The water molecule O35 acts as a donor to water molecule O36. The energy of this and other O–H \cdots O hydrogen bonds were calculated using the correlation from Rammohan and Kaduk (2018). The water molecule O36 acts as a donor to O7, the carbonyl oxygen of the amide group. Both protonated dimethyl amine groups N10 and N9 act as donors in N–H \cdots O hydrogen bonds to the ionized oxygen O6. The energies of these N–H \cdots O hydrogen bonds were calculated using the correlation from

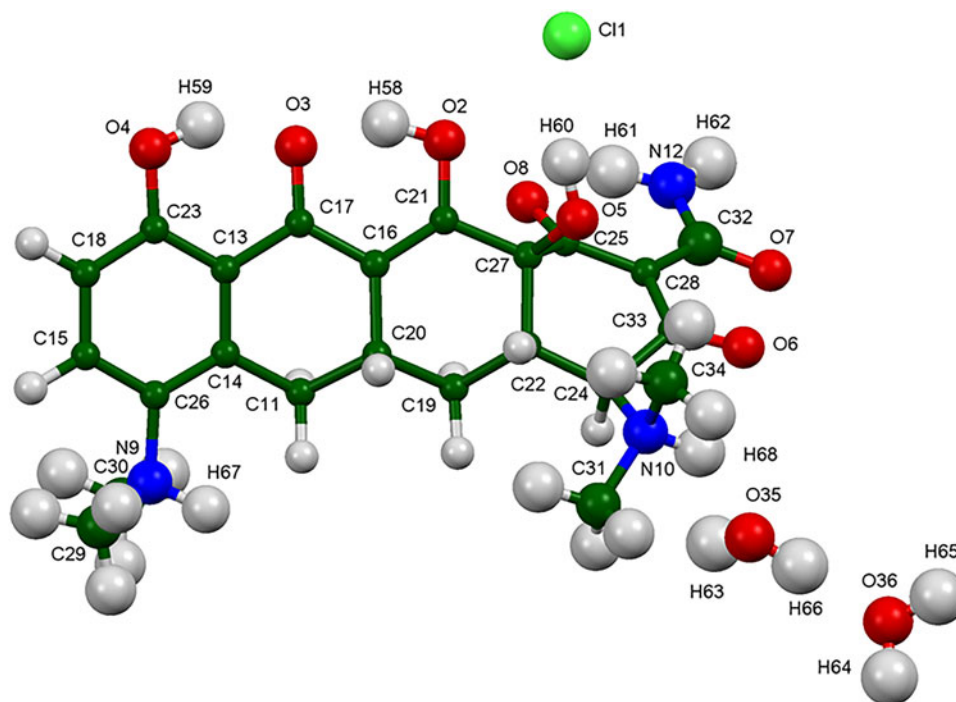


Figure 6. (Color online) The asymmetric unit of minocycline hydrochloride dihydrate, with the atom numbering. The atoms are represented by 50% probability spheroids.

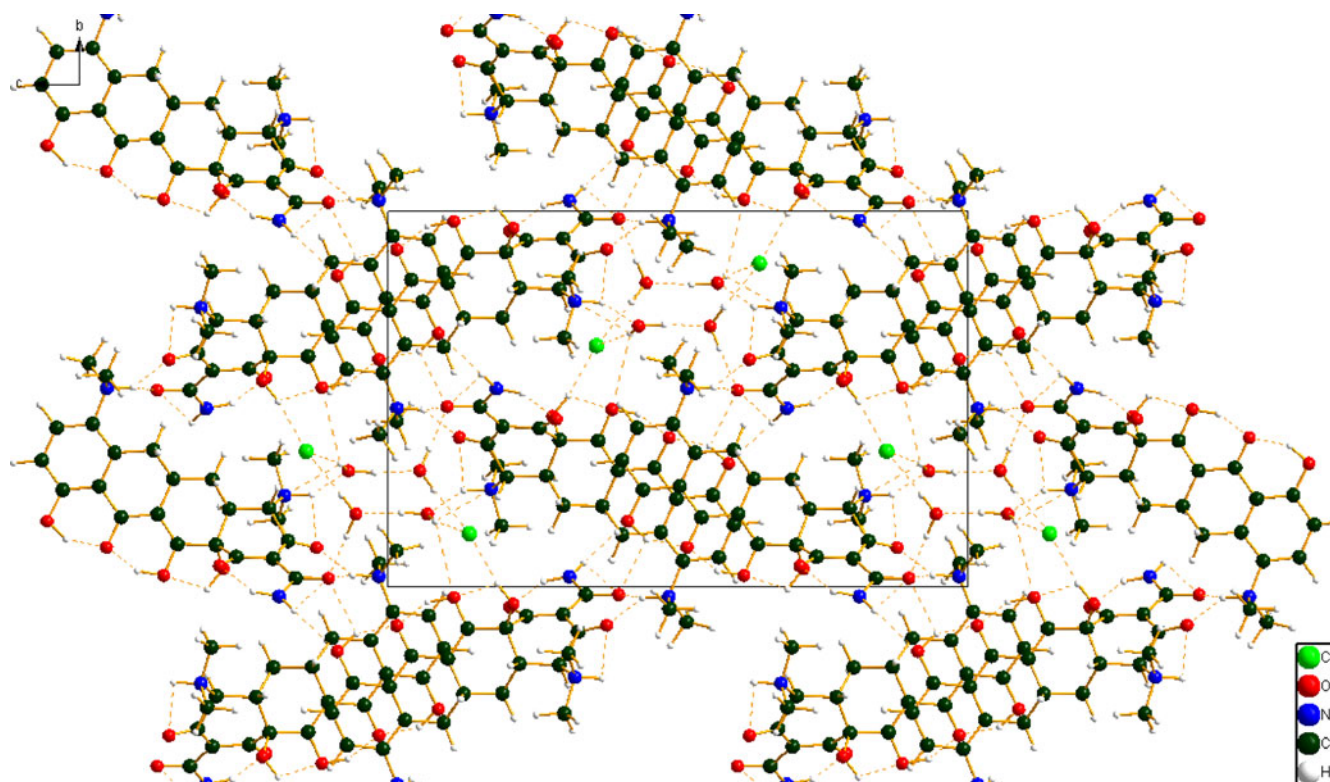


Figure 7. (Color online) The crystal structure of minocycline hydrochloride dihydrate, viewed down the a -axis.

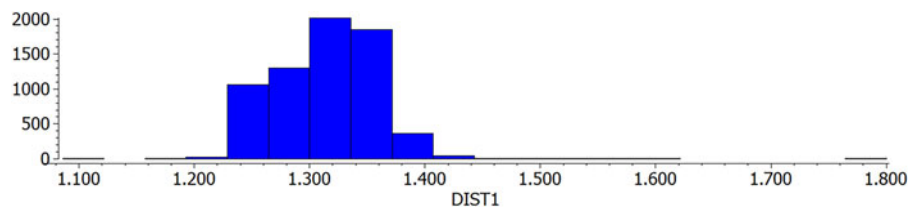


Figure 8. (Color online) Histogram of the phenyl- O^- distances in the Cambridge Structural Database. The C33- O_6 distance (1.254 Å from VASP and 1.247 Å from CRYSTAL14) is smaller than the average phenyl- O^- distance of 1.304(44) Å from 4519 hits in the CSD (Groom *et al.*, 2016). The difference is only -1.2 esd, so the distance is reasonable.

TABLE I. Hydrogen bonds (CRYSTAL14) in minocycline hydrochloride dihydrate.

| H-bond | D-H, Å | H...A, Å | D...A, Å | D-H...Å, | Overlap, e | E, kcal mol $^{-1}$ |
|---------------|--------|----------|----------|----------|--------------|---------------------|
| O35-H66...O36 | 0.984 | 1.781 | 2.764 | 177.4 | 0.062 | 13.6 |
| O35-H63...C11 | 0.974 | 2.358 | 3.299 | 162.3 | 0.027 | 23.1 |
| O36-H65...C11 | 0.977 | 2.308 | 3.274 | 170.2 | 0.034 | 26.0 |
| O36-H64...O7 | 0.982 | 1.863 | 2.838 | 171.5 | 0.055 | 12.8 |
| N10-H68...O35 | 1.041 | 1.913 | 2.834 | 143.6 | 0.055 | 5.4 |
| N10-H68...O6* | 1.041 | 2.155 | 2.600 | 103.2 | 0.026 | 3.7 |
| N9-H67...O6 | 1.042 | 1.790 | 2.653 | 137.5 | 0.047 | 5.0 |
| N12-H62...O4 | 1.009 | 2.272 | 3.052 | 133.2 | 0.015 | 2.8 |
| N12-H61...O8* | 1.017 | 1.898 | 2.695 | 132.9 | 0.054 | 5.4 |
| O5-H60...C11 | 0.978 | 2.395 | 3.303 | 154.3 | 0.020 | 19.9 |
| O5-H60...O2* | 0.978 | 2.308 | 2.747 | 106.2 | 0.009 | 5.2 |
| O4-H59...O3* | 0.995 | 1.680 | 2.546 | 143.0 | 0.055 | 12.8 |
| O4-H59...O7 | 0.995 | 2.444 | 2.982 | 113.4 | 0.019 | 7.5 |
| O2-H58...O3* | 1.009 | 1.557 | 2.483 | 149.6 | 0.079 | 15.3 |
| C24-H45...C11 | 1.098 | 2.384 | 3.464 | 167.4 | 0.018 | |
| C11-H37...O4 | 1.097 | 2.311 | 3.379 | 163.8 | 0.022 | |

*Intramolecular.

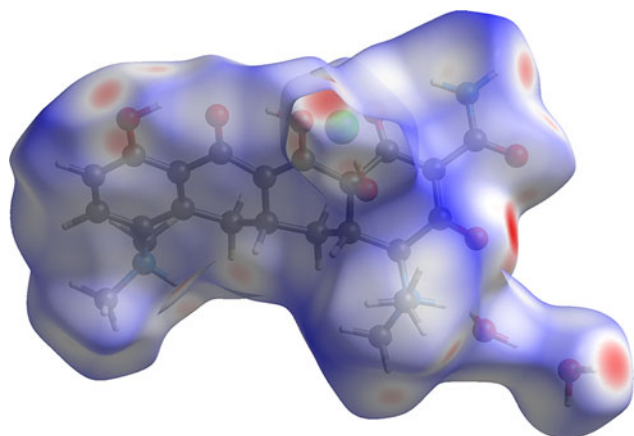


Figure 9. (Color online) The Hirshfeld surface of minocycline hydrochloride dihydrate. Intermolecular contacts longer than the sums of the van der Waals radii are colored blue, and contacts shorter than the sums of the radii are colored red. Contacts equal to the sums of radii are white.

Wheatley and Kaduk (2018). The bond involving N10–H68 is bifurcated both to O6 and the water molecule O35. Both hydroxyl groups O2 and O4 act as donors in intramolecular hydrogen bonds to the carbonyl oxygen atom O3. The hydroxyl group O5–H60 forms bifurcated hydrogen bonds to the chloride anion and (intramolecular) to the hydroxyl oxygen O2. The hydroxyl group O4–H59 also acts as a donor in an intermolecular hydrogen bond to the O7, the carbonyl oxygen atom of the amide group.

The volume enclosed by the Hirshfeld surface (Figure 9; Hirshfeld, 1977; Turner, *et al.*, 2017) is 587.82 Å³, 98.36% of 1/4 the unit cell volume. The molecules are thus not tightly packed. All of the significant close contacts (red in Figure 9) involve the hydrogen bonds.

The Bravais–Friedel–Donnay–Harker (Bravais, 1866; Friedel, 1907; Donnay and Harker, 1937) morphology suggests that we might expect elongated morphology for minocycline hydrochloride dihydrate, with {100} as the long axis. A fourth-order spherical harmonic preferred orientation model was included in the refinement; the texture index was 1.015, indicating that preferred orientation was not significant in this rotated capillary specimen. The powder pattern of minocycline hydrochloride dihydrate from this synchrotron data set is included in the Powder Diffraction File™ as entry 00-066-1606.

SUPPLEMENTARY MATERIAL

The supplementary material for this article can be found at <https://doi.org/10.1017/S0885715618000787>.

ACKNOWLEDGEMENTS

Use of the Advanced Photon Source at Argonne National Laboratory was supported by the US Department of Energy, Office of Science, Office of Basic Energy Sciences, under Contract No. DE-AC02-06CH11357. This work was partially supported by the International Centre for Diffraction Data. The authors thank Lynn Ribaud and Saul Lapidus for their assistance in the data collection, and Andrey Rogachev for the use of computing resources at IIT.

- Altomare, A., Cuocci, C., Giacovazzo, C., Moliterni, A., Rizzi, R., Corriero, N., and Falcicchio, A. (2013). “EXPO2013: a kit of tools for phasing crystal structures from powder data,” *J. Appl. Crystallogr.* **46**, 1231–1235.
- Berman, H. M., Westbrook, J., Feng, Z., Gilliland, G., Bhat, T. N., Weissig, H., Shindyalov, I. N., and Bourne, P. E. (2000). “The protein data bank,” *Nucleic Acids Res.* **28**, 235–242.
- Bravais, A. (1866). *Etudes Cristallographiques* (Gauthier Villars, Paris).
- Bruno, I. J., Cole, J. C., Kessler, M., Luo, J., Motherwell, W. D. S., Purkis, L. H., Smith, B. R., Taylor, R., Cooper, R. I., Harris, S. E., and Orpen, A. G. (2004). “Retrieval of crystallographically-derived molecular geometry information,” *J. Chem. Inf. Sci.* **44**, 2133–2144.
- Dassault Systèmes (2016). *Materials Studio 2017R2* (BIOVIA, San Diego CA).
- Donnay, J. D. H. and Harker, D. (1937). “A new law of crystal morphology extending the law of Bravais,” *Am. Mineral.* **22**, 446–447.
- Dovesi, R., Orlando, R., Erba, A., Zicovich-Wilson, C. M., Civalieri, B., Casassa, S., Maschio, L., Ferrabone, M., De La Pierre, M., D-Arco, P., Noël, Y., Causà, M., and Kirtman, B. (2014). *Int. J. Quantum Chem.* **114**, 1287–1317.
- Favre-Nicolin, V. and Černý, R. (2002). FOX, “free objects for crystallography: a modular approach to ab initio structure determination from powder diffraction,” *J. Appl. Crystallogr.* **35**, 734–743.
- Fawcett, T. G., Kabekkodu, S. N., Blanton, J. R., and Blanton, T. N. (2017). “Chemical analysis by diffraction: the powder diffraction file™,” *Powder Diffr.* **32**(2), 63–71.
- Finger, L. W., Cox, D. E., and Jephcoat, A. P. (1994). “A correction for powder diffraction peak asymmetry due to axial divergence,” *J. Appl. Crystallogr.* **27**(6), 892–900.
- Friedel, G. (1907). “Etudes sur la loi de Bravais,” *Bull. Soc. Fr. Mineral.* **30**, 326–455.
- Gatti, C., Saunders, V. R., and Roetti, C. (1994). “Crystal-field effects on the topological properties of the electron-density in molecular crystals – the case of urea,” *J. Chem. Phys.* **101**, 10686–10696.
- Groom, C. R., Bruno, I. J., Lightfoot, M. P., and Ward, S. C. (2016). “The Cambridge structural database,” *Acta Crystallogr. Sect. B: Struct. Sci., Cryst. Eng. Mater.* **72**, 171–179.
- Hirshfeld, F. L. (1977). “Bonded-atom fragments for describing molecular charge densities,” *Theor. Chem. Acta* **44**, 129–138.
- Kaduk, J. A. (2002). “Use of the inorganic crystal structure database as a problem solving tool,” *Acta Crystallogr. Sect. B: Struct. Sci.* **58**, 370–379.
- Kaduk, J. A., Crowder, C. E., Zhong, K., Fawcett, T. G., and Suchomel, M. R. (2014). “Crystal structure of atomoxetine hydrochloride (Strattera), C₁₇H₂₂NOCl,” *Powder Diffr.* **29**(3), 269–273.
- Kresse, G. and Furthmüller, J. (1996). “Efficiency of Ab-initio total energy calculations for metals and semiconductors using a plane-wave basis set,” *Comput. Mater. Sci.* **6**, 15–50.
- Larson, A. C. and Von Dreele, R. B. (2004). *General Structure Analysis System, (GSAS)*, (Los Alamos National Laboratory Report LAUR 86-784).
- Lee, P. L., Shu, D., Ramanathan, M., Preissner, C., Wang, J., Beno, M. A., Von Dreele, R. B., Ribaud, L., Kurtz, C., Antao, S. M., Jiao, X., and Toby, B. H. (2008). “A twelve-analyzer detector system for high-resolution powder diffraction,” *J. Synchrotron. Rad.* **15**(5), 427–432.
- Macrae, C. F., Bruno, I. J., Chisholm, J. A., Edington, P. R., McCabe, P., Pidcock, E., Rodriguez-Monge, L., Taylor, R., van de Streek, J., and Wood, P. A. (2008). “Mercury CSD 2.0 – new features for the visualization and investigation of crystal structures,” *J. Appl. Crystallogr.* **41**, 466–470.
- Mendes, Z., Antunes, J. R., Marto, S., and Heggie, W. (2010). “Crystalline minocycline base and processes for its preparation,” United States Patent Application 2010/0286417.
- Peintinger, M. F., Vilela Oliveira, D., and Bredow, T. (2013). “Consistent Gaussian basis sets of triple-zeta valence with polarization quality for solid-state calculations,” *J. Comput. Chem.* **34**, 451–459.
- Rammohan, A. and Kaduk, J. A. (2018). “Crystal structures of alkali metal (Group 1) citrate salts,” *Acta Crystallogr. Sect. B* **74**, 239–252.
- Rodrigues, M. A., Tiago, J. M., Padrela, L., Matos, H. A., Nunes, T. G., Pinheiro, L., Almeida, A. J., and Gomes de Azavedo, E. (2014). “New thermoresistant polymorph from CO₂ recrystallization of minocycline hydrochloride,” *Pharm. Res.* **31**, 3136–3149.
- Stephens, P. W. (1999). “Phenomenological model of anisotropic peak broadening in powder diffraction,” *J. Appl. Crystallogr.* **32**, 281–289.

- Sykes, R. A., McCabe, P., Allen, F. H., Battle, G. M., Bruno, I. J., and Wood, P. A. (2011). "New software for statistical analysis of Cambridge structural database data," *J. Appl. Crystallogr.* **44**, 882–886.
- Thompson, P., Cox, D. E., and Hastings, J. B. (1987). "Rietveld refinement of Debye-Scherrer synchrotron X-ray data from Al_2O_3 ," *J. Appl. Crystallogr.* **20**(2), 79–83.
- Toby, B. H. (2001). "EXPGUI, a graphical user interface for GSAS," *J. Appl. Crystallogr.* **34**, 210–213.
- Turner, M. J., McKinnon, J. J., Wolff, S. K., Grimwood, D. J., Spackman, P. R., Jayatilaka, D., and Spackman, M. A. (2017). *CrystalExplorer17* (University of Western Australia): <http://hirshfeldsurface.net>.
- van de Streek, J. and Neumann, M. A. (2014). "Validation of molecular crystal structures from powder diffraction data with dispersion-corrected density functional theory (DFT-D)," *Acta Crystallogr. Sect. B: Struct. Sci., Cryst. Eng. Mater.* **70**(6), 1020–1032.
- Wang, J., Toby, B. H., Lee, P. L., Ribaud, L., Antao, S. M., Kurtz, C., Ramanathan, M., Von Dreele, R. B., and Beno, M. A. (2008). "A dedicated powder diffraction beamline at the advanced photon source: commissioning and early operational results," *Rev. Sci. Instr.* **79**, 085105.
- Wavefunction, Inc. (2017). Spartan '16 Version 2.0.1, Wavefunction Inc., 18401 Von Karman Ave., Suite 370, Irvine CA 92612.
- Wheatley, A. M. and Kaduk, J. A. (2018). "Crystal structures of ammonium citrates," submitted to Powder Diffraction.
- Xiurong, H., Jianming, G., and Linschen, C. (2012). "Minocycline hydrochloride hydrate crystal forms and preparation method thereof," Chinese Patent CN101693669B.